ARTICLE
Journal of Cellular Biochemistry 111:1598–1606 (2010)

Journal of Cellular Biochemistry

C-terminal Domain of p16^{INK4a} is Adequate in Inducing Cell Cycle Arrest, Growth Inhibition and CDK4/6 Interaction Similar to the Full Length Protein in HT-1080 Fibrosarcoma Cells

Najmeh Fahham,[1] Soroush Sardari,[1] Seyed Nasser Ostad,[2] Behrouz Vaziri,[1] and Mohammad Hossein Ghahremani[2*]

[1] *Biotechnology Research Center, Pasteur Institute of Iran, Tehran, Iran*

[2] *Department of Pharmacology–Toxicology, Faculty of Pharmacy, Tehran University of Medical Sciences, Tehran, Iran*

ABSTRACT

The tumor suppressor p16^{INK4a} has earned widespread attention in cancer studies since its discovery as an inhibitor of cyclin-dependent kinases (CDKs) 4/6. Structurally, it consists of four complete ankyrin repeats, believed to be involved in CDK4 interaction. According to the previous disparities concerning the importance of domains and inactivating mutations in p16, we aimed to search for the domain possessing the functional properties of the full length protein. Upon our *in silico* screening analyses followed by experimental assessments, we have identified the novel minimum functional domain of p16 to be the C-terminal half including ankyrin repeats III, IV and the C-terminal flanking region accompanied by loops 2 and 3. Transfection of this truncated form into HT-1080 human fibrosarcoma cells, lacking endogenous p16, revealed that it is able to inhibit cell growth and proliferation equivalent to p16^{INK4a}. The functional analysis showed that this fragment like p16 can interact with CDK4/6, block the entry into S phase of the cell cycle and suppress growth as indicated by colony formation assay. Identification of p16 minimum functional domain can be of benefit to the future peptidomimetic drug design as well as gene transfer for cancer therapy. J. Cell. Biochem. 111: 1598–1606, 2010.

KEY WORDS: P16^{INK4A}; FIBROSARCOMA; CELL CYCLE; ANKYRIN REPEAT; FUNCTIONAL DOMAIN

Cell cycle progression is regulated by complexes formed between cyclins and cyclin-dependent kinases (CDKs). In the G1 phase of the cell cycle, the kinase activity of CDK4 and CDK6 is initiated via association with D-type cyclins [Villacanas et al., 2002]. The function of these G1 kinases is negatively regulated by binding of p16, the founding member of INK4 CDK inhibitors family. Upon binding to the G1 kinases, p16 inhibits the phosphorylation of the retinoblastoma (Rb) protein by CDK4 and CDK6, blocks the activity of E2F transcription factors and the expression of genes essential for the onset of S phase and mitosis, which results in arresting the cells in the G1 phase of the cell cycle [Weinberg, 1995; Classon and Harlow, 2002]. The CDK-cyclin D/p16^{INK4a}/pRb/E_2F cascade has been found to be deregulated in more than 80% of human neoplasias [Paggi et al., 1996; Ortega et al., 2002]. Since it was first reported in 1994, p16^{INK4a} has been considered as one of the most altered genes in a wide variety of malignant human tumors (>70 different types). It has been inactivated by several molecular mechanisms including homozygous deletions, point mutations, and hyper methylation in CpG islands [Herman et al., 1995; Smith-Sorensen and Hovig, 1996; Xie et al., 2005]. Some of these inactivating mutations severely affect the stability of the tertiary structure of p16^{INK4a} and its function [Serrano, 1997].

Structurally, p16 is comprised mainly of four contiguous ankyrin repeats, linear array of a repeating helix-turn-helix structures which are believed to be involved in protein–protein interactions (Fig. 1). The tertiary structure of p16 has a putative cleft for binding to the non-catalytic side of CDK4/6. Upon p16 binding, an allosteric conformational change will be induced in CDK4/6 which in turn decreases their affinity for ATP and D-type cyclins [Pavletich, 1999]. According to the random mutagenesis studies on p16 gene,

Additional supporting information may be found in the online version of this article.

Grant sponsor: Pasteur Institute of Iran.

*Correspondence to: Dr Mohammad Hossein Ghahremani, PhD, Department of Pharmacology–Toxicology, Faculty of Pharmacy, Tehran University of Medical Sciences, Tehran 14155-6451, Iran. E-mail: mhghahremani@tums.ac.ir

Received 20 June 2010; Accepted 20 September 2010 • DOI 10.1002/jcb.22892 • © 2010 Wiley-Liss, Inc.
Published online 4 November 2010 in Wiley Online Library (wileyonlinelibrary.com).

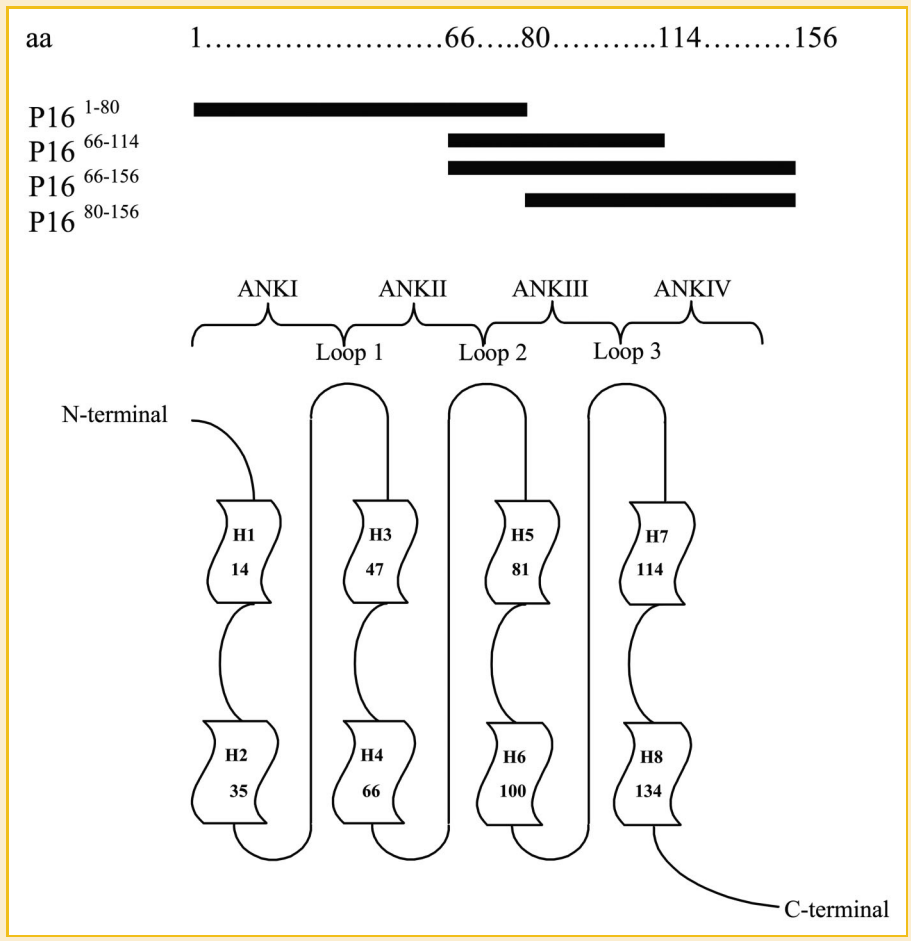

Fig. 1. Topology diagram of p16 structure and schematic representation of ankyrin motifs and loops of four p16 truncated structures evaluated in this study. Each ankyrin repeat exhibits a helix-turn-helix structure. The helices are designated as 1, 2, 3, etc. The four H-T-H motifs are connected by three loops in beta and gamma turn structure [Byeon et al., 1998]. The specifications of construct $p16^{1-80}$, containing the N-terminal part, ANKI, II, loop 1, 2; construct $p16^{66-114}$, containing loop 2, 3, ANKIII; construct $p16^{66-156}$, containing loop 2, 3, ANKIII, IV and the C-terminal part; construct $p16^{80-156}$ containing ANKIII, IV, loop 3 and the C-terminal part are shown. The numbers correspond to the amino acids of p16 full length protein.

there is a large contact surface between p16 and CDK4, while many amino acids throughout the four ankyrin repeats are important for the interaction [Yang et al., 1996]. On the other hand, based on the molecular dynamic studies, some interactions between p16 and CDK4/6 are functionally redundant [Villacanas et al., 2002]. In consistence with these studies, the deletion of C-terminal portion after codon 135 has been shown to have no effect on the activity of p16 *in vitro* [Yang et al., 1995]. Moreover, tumor-associated mutations in the second, third, and early fourth ankyrin repeats occur more frequently at residues that are invariant in all members of the p16 family which results in loss of function; while mutations in the first and late forth ankyrin repeats are less likely to disrupt p16 function [Yarbrough et al., 1999]. Detailed structural analysis has shown that mutations are present with high frequency in three regions: loop 2, entire ANKIII, and from loop 3 to the beginning of helix IVB [Byeon et al., 1998]. Regarding the importance of ANKIII, it has been proposed that a short 20-residue peptide derived from this ankyrin repeat with the same sequence as fragment 84-103 of p16 can be selected for its ability to bind and inhibit CDK4 *in vitro* [Fahraeus et al., 1996].

Along with the ankyrin repeats that are important motifs in protein–protein interactions, the contribution of the loops to interaction with CDK4/6 cannot be denied although they show less defined structure due to the conformational flexibility in p16 [Byeon et al., 1998; Li et al., 1999].

In this study, to evaluate the functional region of p16, we have generated different truncated structures (including different ankyrin motifs and loops) based on our previous *in silico* screening of the eight truncated forms regarding their interaction with CDK4 [Fahham et al., 2009]. The effect of the generated truncated structures on growth inhibition and cell cycle were then evaluated in HT-1080, p16-deficient and wild type pRb fibrosarcoma cell line [Li et al., 1995; Whitaker et al., 1995; Roninson, 2003]. The results reported here, indicate that p16 C-terminal half including ANKIII and IV together with loop 2 and 3 can efficiently behave similar to the full length p16, providing a functional domain as a therapeutic target for blocking CDK4/6 in cancer cells.

MATERIALS AND METHODS

CELL LINES AND CULTURE CONDITIONS

The human fibrosarcoma cell line, HT-1080 (p16 null) (National Cell Bank of Iran, Pasteur Institute of Iran) was maintained in RPMI-1640 medium (BioSera, UK) supplemented with 10% fetal bovine serum, 100 units/ml penicillin and 100 μg/ml streptomycin (all from Gibco, UK) at 37°C in humidified incubator containing 5% CO_2.

PCR AND PLASMIDS CONSTRUCTION

The human p16 wild type gene was purchased from Genecopoeia (USA). Four truncated constructs, named $p16^{1-80}$, $p16^{66-114}$, $p16^{66-156}$, and $p16^{80-156}$ (Fig. 1), were generated by PCR using specific primer pairs carrying restriction enzyme sites and cloned into pcDNA3.1 mammalian expression vector (Table I). For proper expression, the ATG, Kozak sequence and the stop codon were engineered in the constructs. The truncated forms were amplified in a 50 μl reaction mixture containing 100 ng p16 gene, 10 pmol of each primer, 0.2 mM dNTP, 1.5 mM $MgCl_2$, 0.5 U Taq polymerase, 1 × PCR buffer (all from CinnaGen, Iran) and 5% DMSO using the following touchdown PCR conditions: 10 cycles of 94°C for 30 s, 65–0.5°C per cycle for 45 s, 72°C for 30 s, 25 cycles of 94°C for 2 min, 60°C for 30 s, 72°C for 30 s followed by a final 5 min extension at 72°C. The reactions were verified on a 1.5% agarose gel by ethidium bromide staining and the sequences were confirmed by DNA sequence analysis. The gel extracted products were then cloned into pcDNA3.1 Myc/His (Invitrogen, USA) according to their restriction sites. The G construct was prepared carrying a flag tag at its C-terminus.

TRANSIENT TRANSFECTION, CELL GROWTH SUPPRESSION AND MTT ASSAY

For cell viability assays, HT-1080 cells were seeded in 24-well tissue culture plate in triplicate 24 h before transfection. At 60–70% confluence, transfection was performed with 2 μg of pcDNA3.1 (vector control), p16 and its four truncated forms using FuGENE® 6 transfection reagent (Roche, Germany) according to the manufacturer's instructions. 24–48 h after transfection, the cells were harvested and counted using trypan blue dye exclusion method. The cytotoxicity was measured by MTT assay 24–48 h after transfection using tetrazolium salt (Sigma, UK). Dye conversion was measured at 570 nm using microplate reader. Each assay was completed in triplicate and the results of three independent experiments were reported.

RT-PCR ANALYSIS

Total RNA was extracted from HT-1080 cells using RNeasy mini kit (Qiagen, Germany) or Tripure reagent (Roche, Germany) 24 h after transfection. In order to eliminate the genomic and plasmid DNA contaminations, the extracted RNAs were treated with DNase I (Qiagen, Germany) in 37°C for 30 min which afterwards incubated at 65°C for 5 min in the presence of 25 mM EDTA to inactivate the DNase I. One microgram of RNA was reverse-transcribed using M-MLV Reverse Transcriptase (Fermentas, Ukraine). Expression analysis of p16 and the four truncated constructs was performed in a 25 μl reaction mixture using 1 μl cDNA, 10 pmol of each primer, 0.2 mM dNTP, 1.5 mM $MgCl_2$, 0.5 U Taq polymerase, 1 × PCR buffer and 1% Q-solution (Qiagen, Germany). PCR amplification was performed under the following conditions: 20 cycles of 94°C for 30 s, 65–0.5°C per cycle for 45 s, 72°C for 30 s, 20 cycles of 94°C for 2 min, 55°C for 30 s, 72°C for 30 s followed by a final 5 min extension at 72°C. β-actin was used as the internal control and amplified with the same condition.

CELL CYCLE ANALYSIS

At 24 h after transfection of the constructs including the pcDNA3.1 empty vector, HT-1080 cells were trypsinized and washed once with PBS and resuspended in hypotonic fluorochrome solution containing 50 μg/ml propidium iodide DNA staining buffer (Sigma, Germany). After incubation for 3 h at 4°C, the cell cycle distribution was recorded in FL3 using fluorescence-activated cell-sorting (FACS; Becton Dickinson, Heidelberg, Germany).

IMMUNOBLOTTING

Cellular protein extract was prepared 24–48 h after transfection by resuspending the cell pellets in lysis buffer containing 30 mM Tris-HCl (pH 7.4), 150 mM NaCl, 1% Triton X-100, 10% glycerol, 1 μM sodium orthovanadate, 5 mM sodium fluoride, 1 mM β-glycerophosphate including 2 mM dithiothreitol (DTT), 200 μM PMSF and 1× protease inhibitor cocktail (Roche, Germany). The cell extracts were separated on 12–17% SDS–polyacrylamide gel electrophoresis and blotted using nitrocellulose membrane (Amersham, Germany). The membranes were then blocked for 1 h in 5% non-fat dried milk in PBS and 1% Tween 20 at room temperature and probed with primary antibodies for 16–20 h at 4°C as follows: Flag M_2 (F3165, Sigma), Myc (C3956, Sigma), human p53 (610183, BD Transduction), Mcl-1 (AAP-240, Stressgen), Bcl2 (51-6511 GR, PahrMingen), Bim (2819, Cell Signaling), Puma (p 4743, Sigma), Noxa (114C307-1, Alexis), p21 (556431, Pharmingen). After washing the blots with PBST for three times, the bands were visualized using horseradish peroxidase

TABLE I. The Primers and Cloning Sites Used to Construct p16 Truncated Forms

Construct	Primer pairs	Cloning site	Product size (bp)
$p16^{1-80}$	*For*: TTGAAGGAATTCGGTACCATGGAGCCG	KpnI	345
	Rev: CGTCGTGCTCGAGTCGGGTGAGAGTG	XhoI	
$p16^{66-114}$	*For*: GGCGGAGAAGCTTGCGATGCACG	HindIII	247
	Rev: CCAGCTCGAGGGGCAGACGGC	XhoI	
$p16^{66-156}$	*For*: GAGGAATTCACCATGCACGGCGC	EcoRI	327
	Rev: TATGCGGCCGCTCACTTGTCGTC	NotI	
$p16^{80-156}$	*For*: CGCCAAGCTTACCATGCGACCCGTGC	HindIII	322
	Rev: CCTCTAGAATCGGGGATGTCTGAGGG	XbaI	

conjugated secondary antibody (Santa Cruz, Germany) and the ECL chemiluminescence detection system (Amersham Bioscience, Germany).

IMMUNOFLUORESCENT STAINING

Cells grown on coverlips were fixed with 3.7% paraformaldehyde, permeabilized with 0.1% Triton X-100, and stained with mouse anti-Myc monoclonal antibody (1:150; Invitrogen) overnight. The slides were then incubated with goat anti-mouse IgG-FITC (1:200) for an additional hour at 4°C, mounted using Vectashield mounting medium for immunofluorescence (Vector Laboratories) and analyzed by an electron scanning confocal microscope (Leica, Bensheim, Germany) and the software supplied by the manufacturer.

IMMUNOPRECIPITATION

At 24–48 h after transfection, cells were lysed in ELB (50 mM HEPES, pH 7.0, 0.1% Nonidet p-40, 250 mM NaCl, 5 mM EDTA, 2 mM DTT and 1× protease inhibitor cocktail (Roche, Germany) for 10 min on ice and clarified by centrifugation at 14000 × g for 10 min. One milligram of protein extract was imunoprecipitated with 2 μl of Flag M_2 antibody (F3165, Sigma, Germany) at 4°C over night followed by capturing with Dynabeads pan mouse IgG (Invitrogen, Germany) for 2 h at 4°C. All immunoprecipitations were washed three times in ELB prior to further manipulation. Labeled proteins were resolved on SDS polyacrylamide gels and subjected to primary antibodies against CDK4 (sc-260, Santa Cruz) and CDK6 (sc-7961, Santa Cruz). Immunodetection was carried out as described above.

COLONY FORMING ASSAY

HT-1080 cells were harvested 48 h after transfection and 5000 cells were seeded in 6 well culture plates. Being incubated for 24 h, the cells were subjected to selection with 1 mg/ml of G418 (Roche, Germany) and allowed to develop colonies for 2 weeks. The colonies were fixed with 10% paraformaldehyde and stained with 0.5% crystal violet. Colony numbers larger than 1 mm in diameter were counted.

STATISTICAL ANALYSIS

Data on cell proliferation were analyzed by one-way ANOVA followed by Tukey post-test and $P \leq 0.05$ was considered statistically significant. All the experiments were performed in triplicate and the results of the three independent experiments were reported as Mean ± SE.

RESULTS

GENERATION OF THE CONSTRUCTS

According to the *in silico* interaction studies of p16 truncated forms and CDK4 [Fahham et al., 2009], four truncated forms (including the ATG and the stop codon) were constructed by PCR-based amplification with four pairs of primers (described in Table I) using p16 full length. Figure 1 shows the schematic presentation of the ankyrin repeats and the loops included in each construct. The constructs were then cloned in pcDNA3.1 expression plasmid as myc or flag-tagged (Suppl. Fig. 1).

EFFECTS OF EXOGENOUS EXPRESSION OF P16 FULL LENGTH AND THE FOUR TRUNCATED FORMS ON THE CELL GROWTH AND CELL VIABILITY

Prior to the cellular assays, transfection efficiency was optimized by introduction of pEGFPN1 vector into the HT-1080 cells. FACS analysis was performed to determine the percentage of GFP-expressing cells representing the efficiency (data not shown), the best of which was used for the experiments afterwards. The obtained results indicated that full length p16 can remarkably reduce cell counts (44.6%) at 24 h which was consistent until 48 h compared to the mock group (vector transfected cells). Among the four truncated forms ($p16^{1-80}$, $p16^{66-114}$, $p16^{66-156}$, and $p16^{80-156}$), the expression of $p16^{66-156}$ construct demonstrated comparable results to that of

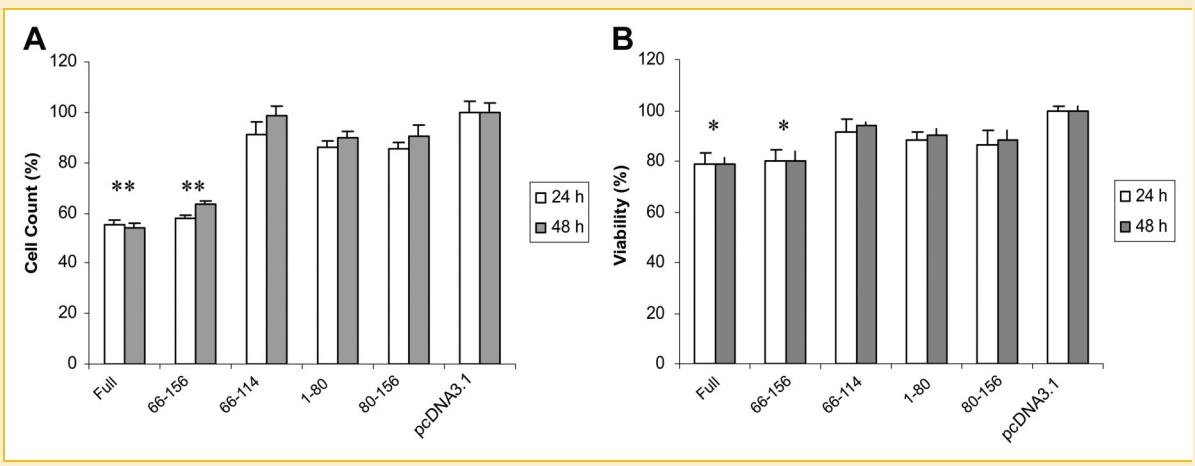

Fig. 2. Effect of p16 and its four truncated forms on the growth and viability of HT-1080 cell line. Cells were transfected with full length p16 (full) and the truncated forms ($p16^{66-156}$, $p16^{66-114}$, $p16^{1-80}$ and $p16^{80-156}$). Cell proliferation was determined by live cell count using trypan blue (A); cell viability was measured by MTT assay (B) as described in the methods. Data were calculated as percent control compared to the vector transfected (pcDNA3.1) group. The results from three independent experiments were presented as Mean ± SE (n = 3, $^{*}P < 0.05$, $^{**}P < 0.01$).

full length p16, (42% growth inhibition at 24 h compared to the control group, $P < 0.01$, Fig. 2A). Consistently, the results from the MTT assay were identical to the cell counting data. While HT-1080 cells expressing full length p16 as well as $p16^{66-156}$ truncated form had remarkably lower viability, there was no significant difference in the mean uptake of the cells transfected with the other truncated forms compared to the control group (Fig. 2B). These results show that $p16^{66-156}$ truncated form similar to p16, can act as an inhibitor of cell growth.

EXPRESSION OF P16 AND THE TRUNCATED FORMS BY RT-PCR AND WESTERN BLOT ANALYSIS

Expression of p16 and the four truncated forms at mRNA level were confirmed 24 h after transfection in HT-1080 cells by RT-PCR as described above. The fragments sizes were as expected. β-actin was used as the internal control (Fig. 3A).

Protein expression of p16 and the truncated forms were analyzed 24 h after transfection by immunoblotting (Fig. 3B). As demonstrated, the cells transfected with p16 full length, $p16^{66-156}$ and $p16^{80-156}$ constructs are expressing high levels of protein. However, we did not detect the expression of $p16^{1-80}$ and $p16^{66-114}$ fragments after transfection. We were able to verify translation of $p16^{80-156}$ and $p16^{1-80}$ constructs by imnunofluorescent staining. As shown in the Figure 3C, while strong expression of $p16^{80-156}$ truncated form is shown in the transfected cells, a weak signal is detected in structure $p16^{1-80}$ and no signal in structure $p16^{66-114}$ transfected cells despite positive expression at mRNA level.

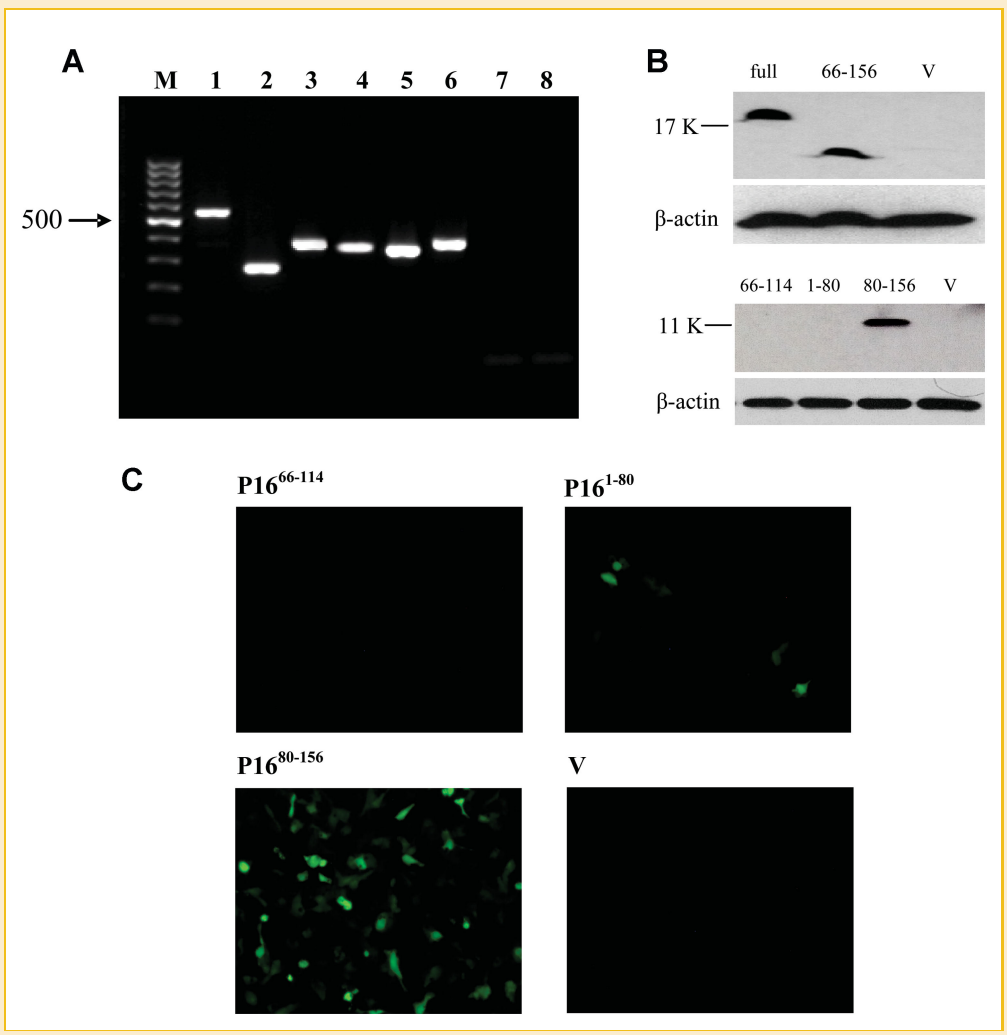

Fig. 3. Expression of p16 and its truncated forms. HT-1080 cells were transfected with p16 and the truncated forms and the cells were harvested and subjected to expression analysis 24 h after transfection as described in the methods (A) mRNA expression was evaluated by RT-PCR analysis; p16 full length (lane 1), $p16^{66-114}$ truncated form (lane 2), $p16^{1-80}$ truncated form (lane 3), $p16^{80-156}$ truncated form (lane 4), $p16^{66-156}$ truncated form (lane 5), β-actin (lane 6), pcDNA3.1 empty vector (lane 7) and RT-PCR negative control (lane 8). (B) Protein expression was evaluated by immunoblotting in cells transfected with p16 (full) or $p16^{66-156}$ (66-156) truncated from (both tagged with Flag epitope), $p16^{66-114}$ (66-114), $p16^{1-80}$ (1-80), and $p16^{80-156}$ (80-156) truncated forms (tagged with myc epitope) using Flag and myc antibody respectively. Empty vector transfected cells (pcDNA3.1) were used as the negative control. (C) Immunoflourescent staining of HT-1080 cells after transfection with $p16^{66-114}$, $p16^{1-80}$ and $p16^{80-156}$ truncated forms compared to pcDNA3.1 as vector control (V) with anti-Myc monoclonal antibody. Positive expression of $p16^{80-156}$ truncated construct and weak expression of $p16^{1-80}$ truncated form is demonstrated whereas no signal is detected in $p16^{66-114}$ transfected cells. [Color figure can be viewed in the online issue, which is available at wileyonlinelibrary.com.]

TABLE II. Cell Cycle Distribution Following p16 and the Four Truncated Forms Expression

	Vector	p16	$p16^{66-114}$	$p16^{1-80}$	$p16^{80-156}$	$p16^{66-156}$
G_0/G_1	48.64 ± 3.3	70.58 ± 1.3*	45.5 ± 3.1	47.97 ± 3.6	54.29 ± 3.3	62.14 ± 2.1*
S	31.27 ± 4.6	14.78 ± 4.1*	28.8 ± 5.0	28.34 ± 4.0	24.28 ± 0.6	21.95 ± 2.6*
G_2	18.42 ± 5.9	14.33 ± 3.6	25.2 ± 1.3	23.07 ± 5.4	19.63 ± 4.3	15.02 ± 2.8

Cell cycle profiles were determined by PI staining 24 h after transfection. Indicated is the percentage of cell population in each phase reported as Mean ± SD of three independent experiments (n = 3, $^*P < 0.05$).

CELL CYCLE REDISTRIBUTION FOLLOWING ECTOPIC EXPRESSION OF P16 AND ITS FOUR TRUNCATED FORMS

To examine the effect of p16 and the truncated forms expression on cell cycle entry, HT-1080 transfected cells were harvested 24 h post transfection and subjected to FACS measurement as described above. Flow cytometric analysis revealed that p16 expression can result in a significant accumulation of cells in G_0/G_1 phase and decreased cell population in S phase relative to the vector control (Table II). The related G_1 arrest correlated directly with the expression status of p16, while reduced p16 expression at 72 h led to the restoring of the cell cycle profile. Interestingly, among the truncated forms, $p16^{66-156}$ construct could function almost similarly to p16 wild type in arresting the G_0/G_1 phase progression in a significant manner at 24 h. None of the other truncated forms altered the cell cycles in transfected cells.

EFFECT OF P16 AND THE TRUNCATED FORMS EXPRESSION ON COLONY FORMATION IN HT-1080 CELLS

To further examine the capability of p16 and the truncated forms on arresting the growth of p16 negative HT-1080 cells, colony forming assay was performed. As illustrated in Figure 4, p16 expression almost completely blocked colony formation in HT-1080 cells compared to the vector transfected group ($P < 0.01$). The cells expressing $p16^{66-156}$ truncated form inhibited colony formation (85%, $P < 0.01$) comparable to that of p16 full length, whereas other constructs did not cause any inhibition of colony formation. These data suggest that $p16^{66-156}$ truncated form acts as a potent regulator of cell growth similar to the full length p16.

EVALUATION OF P16 AND $P16^{66-156}$ TRUNCATED FORM BINDING TO CDK4 BY IMMUNOPRECIPITATION

Since p16 is known to regulate the cell cycle by interaction with CDK4/6 we evaluated the physical interaction of p16 and G truncated form with CDK4 by immunoprecipitation. Therefore, cell lysates of HT-1080 cells transfected with p16, $p16^{66-156}$, and pcDNA3.1 plasmids were immunoprecipitated with anti-flag antibody and probed for CDK4 and CDK6 by western blot analysis. As illustrated in Figure 5, p16 and $p16^{66-156}$ truncated form interact well with both CDK4 and CDK6, demonstrating that $p16^{66-156}$ construct is capable of binding to CDK4/6 similar to p16 full length.

EFFECT OF P16 AND G TRUNCATED FORM ECTOPIC EXPRESSION ON THE LEVEL OF PRO- AND ANTI-APOPTOTIC PROTEINS

To address whether expression of p16 and $p16^{66-156}$ truncated form may have any influence on the level of other proteins involved in proliferation or apoptosis, whole cell lysates of p16 and $p16^{66-156}$ transfected cells were prepared 24 and 48 h after transfection and immunoblotted against Mcl-1, Bcl2, Bim, Puma, Noxa, and p21. As shown in Figure 6, p16 and $p16^{66-156}$ expression were found to down-regulate Mcl-1 at 24 h and Bcl2 at 48 h after transfection.

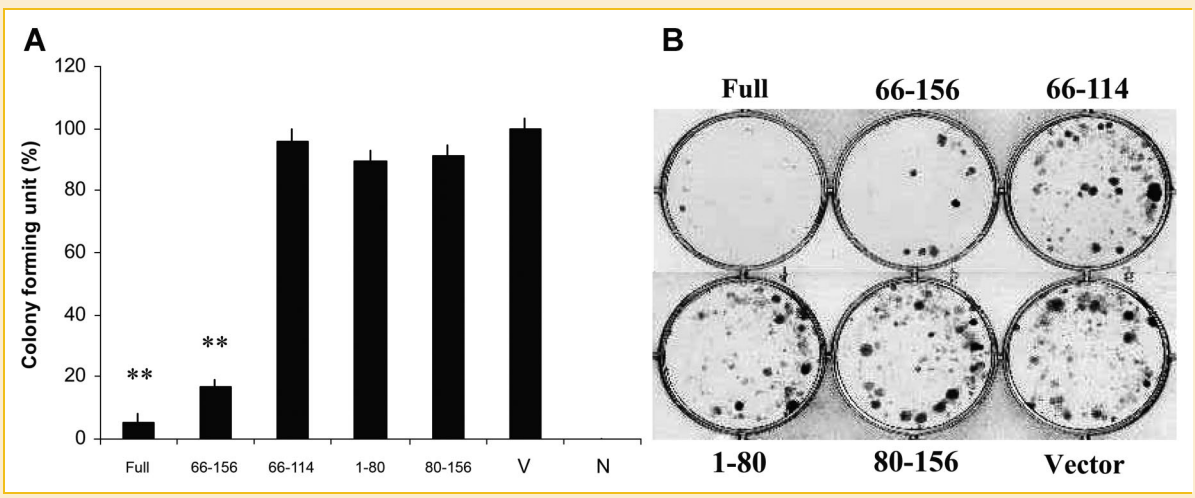

Fig. 4. Effect of p16 and the truncated forms on colony formation in HT-1080 cells. The cells were transfected with p16 full length (full), $p16^{1-80}$, $p16^{66-114}$, $p16^{66-156}$, $p16^{80-156}$, and pcDNA3.1 empty vector and the resistant colonies were selected with 1 mg/ml G418 for 2 weeks. (A) Data are presented as mean ± SD of percent colony formation relative to pcDNA3.1 based on three independent experiments (n = 3). (B) The representative of the colonies stained with crystal violet.

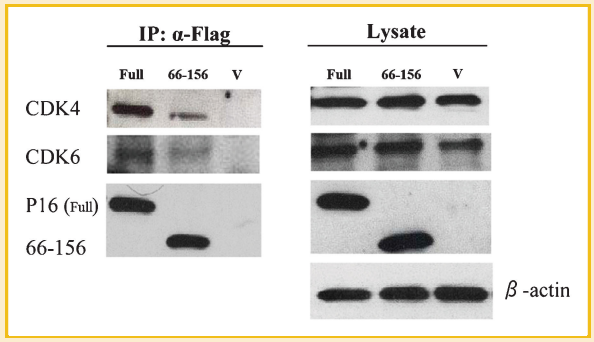

Fig. 5. Protein interaction of p16 full length (full) and $p16^{66-156}$ (66–156) truncated form with CDK4 and CDK6 compared to vector (V) transfected cells. Flag tagged p16 and $p16^{66-156}$ truncated form were transfected into HT-1080 cells and the cell lysate was immunoprecipitated with anti-flag antibody and probed for CDK4 and CDK6. As indicated, flag tagged p16 and $p16^{66-156}$ truncated form interact with CDK4 and CDK6.

Moreover, protein levels of Bim and p21 were clearly up regulated within 24 and 48 h respectively. There was a slight increase in the amount of Puma and Noxa after 24 h. These results demonstrate that ectopic expression of $p16^{66-156}$ truncated form induces changes in the cellular protein levels similar to p16 wild type.

DISCUSSION

Advancement from the early G_1 phase of the cell cycle into the late G_1 phase requires the activity of several cyclin-CDK complexes which can be inhibited by p16 tumor suppressor. Over expression of p16 in several tumor types has been shown to inhibit cell proliferation and induce cell cycle arrest in several studies [Frost et al., 1999; McConnell et al., 1999; Ramirez et al., 2001]. Furthermore, progress has been made with several studies establishing a role for p16 in cell senescence, anoikis, cell spreading, and angiogenesis [Fahraeus and Lane, 1999; Harada et al., 1999; Plath et al., 2000]. It has been shown that p16 protein interacts with CDK4/6 via its ankyrin repeats and mutation in these regions affects the cell cycle arrest function [Yang et al., 1996; Byeon et al., 1998]. However, only few attempts have been made to explore p16 functional domains.

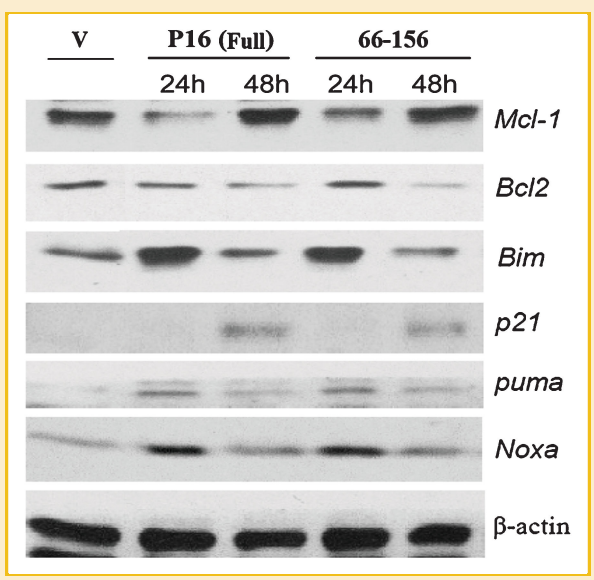

Fig. 6. Effect of p16 full length (full) and $p16^{66-156}$ (66–156) truncated from on expression of pro and anti-apoptotic proteins. HT-1080 cells were transfected with p16 and $p16^{66-156}$ truncated form and the cell lysates were prepared at 24 and 48 h and probed for specific antibodies against Mcl-1, Bcl2, Bim, p21, Puma, and Noxa. β-actin served as a loading control.

Due to the large contact surface between p16 and CDK4/6 according to the crystal structures and the molecular dynamics achievements [Villacanas et al., 2002] and disparities among several reports concerning the loss-of-function mutations throughout the protein, it is difficult to confine the interaction to one ANK motif or one loop. Moreover, previous proteolysis and deletion studies suggest that individual ANK repeats cannot fold independently [Michaely and Bennett, 1993]. Therefore, it had to be considered that a minimal number of ankyrin repeats is required to provide stabilizing interactions between the helices and the loops in the ankyrin repeat structures [McDonald and Peters, 1998]. In this regard, it would be appealing to determine whether different truncations have any effect on the properties of the protein.

In an attempt to identify the minimum stable and functionally active region of p16, the preliminary investigation was performed *in silico* in our team [Fahham et al., 2009]. In this regard, the protein was sequentially divided into smaller building blocks and eight truncated structures were created by homology modeling pertaining to the most critical regions of p16 for interaction and inhibition of CDK4 according to the previous investigations [Yang et al., 1995; Tevelev et al., 1996; Yang et al., 1996; Yarbrough et al., 1999]. Based upon this study, four truncated forms were selected to be characterized according to their mode of effect on growth inhibition of HT-1080 human fibrosarcoma cells. HT-1080 cells are deficient in p16 expression [Roninson, 2003] and positive for Rb and p53 [Li et al., 1995] and there has been no previously published data considering the effect of ectopic expression of p16 in this cell line.

Enforced expression of p16 in HT-1080 cells significantly reduced cell proliferation and viability, induced cell cycle arrest, and inhibited colony formation efficiency. Intriguingly, $p16^{66-156}$ truncated construct, harboring loop 2, 3, ANKIII, IV and the C-terminal segment, possess almost the same function comparable to p16 among the truncated forms. The mechanism responsible for the decrease in cell proliferation was related to the shifting of the cell population into the G_1 phase of the cell cycle. This effect was dependent directly on the expression status of p16, since reduced p16 expression at 72 h led to the restoring of the cell cycle profile. Our findings indicated that $p16^{66-156}$ truncated form was able to physically interact with CDK4, though with a weaker affinity to that of p16 wild type. It has been previously observed that p16 induction can cause some alterations in the expression of pro and anti-apoptotic proteins such as Noxa, puma, Mcl-1, and Bcl2 in T-cell leukemia [Obexer et al., 2009]. Expression of $p16^{66-156}$ truncated form similar to the full length p16 was capable of repressing Mcl-1 and Bcl2 and induction of p21, puma, Noxa, and Bim protein levels

in our investigations. These findings suggest that $p16^{66-156}$ truncated form can function as good as the full length protein in inhibiting the tumor cell proliferation.

Based upon the previous reports, p16 is extremely vulnerable to mutations, resulting in aggregation and loss of activity [Tang et al., 1999]. In particular, it is proposed that most residues with high backbone flexibility are clustered in the N-terminal half of p16 which make it significantly more sensitive to proteolysis than the wild type suggesting that this region is particularly unstable [Yuan et al., 1999; Zhang and Peng, 2002]. Consistent with this report, it is showed that p16 unfolds in a sequential and directional manner; first the two N-terminal repeats and then the two C-terminal regions (repeats III and IV), which appear to be more rigid and serve as a structural scaffold for the folding of the whole protein [Tang et al., 2003]. Most notably, Zhang and Peng [2000] have defined the smallest ankyrin repeat module to be the C-terminal half, consisting of the third and fourth ankyrin repeats of p16 (structures $p16^{66-156}$ and $p16^{80-156}$ in our study) that can fold autonomously into a native-like structure similar to p16. However, they were unable to express the N-terminal half of p16, consisting of the first and second ANK repeats confirming the instability and inability of this region to fold independently.

Likewise, we were also unable to detect the protein expression of $p16^{66-114}$ (containing loop 2, 3, ANKIII) and $p16^{1-80}$ (containing the N-terminal part, ANKI, II and loop 1, 2) truncated structures by immunoblotting and we obtained a week signal for $p16^{1-80}$ and no signal for $p16^{66-114}$ truncated form according to immunoflourescent staining results. This can be possibly due to the decreased stability and ease of degradation of these fragments as discussed above. Furthermore, it is previously observed that individually expressed ANKIII and IV are unstructured in solution and presence of both ANK repeats and the covalent linkage between them is necessary for the proper and independent folding [Tang et al., 2003]. It should be mentioned that the mRNA expression of $p16^{66-114}$ and $p16^{1-80}$ truncated forms was confirmed by RT-PCR analysis. Lack of expression and/or protein instability may render these truncated forms functionally impaired in inhibition of proliferation and cell cycle progression.

On the other hand, it has been reported that a synthetic 20-residue peptide (corresponding to residues 84-103 of wild type p16) can mimic the function of p16 both *in vitro* and *in vivo* when it is coupled to a small carrier peptide and applied directly to the culture medium [Fahraeus et al., 1996]. The $p16^{66-114}$ construct (amino acids 66–114) in our study includes all these residues; however it did not reflect any changes in cell proliferation or colony formation. This discrepancy may result from the different introduction of these fragments to the cells, as we have used gene transfection of the construct, while the other group has added the prepared carrier-linked peptide to the medium. Upon expression, $p16^{66-114}$ construct may undergo proteolytic degradation due to its unstructured status, whereas the 20-residue synthetic peptide will translocate through the membrane directly and consequent to binding to CDK4 it possibly adopts a conformation that blocks the catalytic side of the kinase [Zhang and Peng, 2000].

According to our data, it is concluded that presence of loop 2 is extremely important for CDK4/6 interaction together with cell cycle and proliferation inhibition. Although truncated structures $p16^{66-156}$ and $p16^{80-156}$ are just different in the presence of loop 2, they represented a different picture in our experiments. In this regard, $p16^{66-156}$ construct appeared to behave similar to the wild type p16 in all of the performed functional and biological assays, while $p16^{80-156}$ construct had only a marginal effect on cellular proliferation and no effect on cell cycle profile and colony forming efficiency despite appropriate protein expression confirmed by western blot analysis implying the proper folding and stability of this fragment.

Although the loops are poorly structured compared with the helical ANK segments in p16, it has been suggested that loops or the tips of the loops are the possible sites for ankyrin-repeat-containing proteins interactions including the interaction between p16 and CDK4 [Batchelor et al., 1998; Baumgartner et al., 1998; Byeon et al., 1998]. In this respect, the contribution of loop 1 and 2 of p16 to the CDK6 binding has been notified more than loop 3 [Russo et al., 1998]. Furthermore, Li et al. [1999] have highlighted the importance of loop 2 in interaction and function of p16 through mutational analysis.

Along with loop 2, truncated structure $p16^{66-156}$ embraces other critical residues for CDK4 interaction like Phe^{90}; Glu^{88}, Gly^{89}, Asp^{92}, and Asp^{84} that have roles in selectivity toward CDK4/6, distortion of the ATP-binding site and binding to CDK4 respectively [Villacanas et al., 2002]. Moreover, this fragment includes the highest frequency regions considering the inactivating mutations corresponding to residues 71–76, 80–102, and 107–127 [Byeon et al., 1998]. It seems that the presence of ANKIV as well as the C-terminal part, although outside the interaction sites and not critical for p16 function [Koh et al., 1995; Tevelev et al., 1996], may influence the stability and conformation of the remainder part of fragment $p16^{66-156}$ in a way that makes it appropriate for CDK4 binding and inhibition. There is an evidence implying that deletion of the C-terminal residues or removal of the fourth ankyrin repeat has enhanced the tendency of p16 for aggregation and abolished CDK binding [Parry and Peters, 1996; Tevelev et al., 1996; Yang et al., 1996].

According to our findings, analysis of different truncated forms of p16 revealed an association between their structure and biological/biochemical activities and showed that the *in silico* predictions fit well with our experimental study results.

Taken together, we have reported the identification and functional characterization of a novel minimum functional domain of p16, possessing amino acids 66–156 which behaves indiscernible from wild type p16 in cell cycle arrest, cell growth inhibition, and CDK interaction. This functional domain can serve as a template for drug discovery or used as a therapeutic agent to block cell proliferation in cancer cells.

ACKNOWLEDGMENTS

The authors thank Dr Mike-Andrew Westhoff and Dr Michael J. Ausserlechner for their scientific advice and Mr H. Akbari for technical assistance. This study was supported by a grant from Pasteur Institute of Iran.

REFERENCES

Batchelor AH, Piper DE, de la Brousse FC, McKnight SL, Wolberger C. 1998. The structure of GABPalpha/beta: an ETS domain- ankyrin repeat heterodimer bound to DNA. Science 279:1037–1041.

Baumgartner R, Fernandez-Catalan C, Winoto A, Huber R, Engh RA, Holak TA. 1998. Structure of human cyclin-dependent kinase inhibitor p19INK4d: comparison to known ankyrin-repeat-containing structures and implications for the dysfunction of tumor suppressor p16INK4a. Structure 6:1279–1290.

Byeon IJ, Li J, Ericson K, Selby TL, Tevelev A, Kim HJ, O'Maille P, Tsai MD. 1998. Tumor suppressor p16INK4A: determination of solution structure and analyses of its interaction with cyclin-dependent kinase 4. Mol Cell 1:421–431.

Classon M, Harlow E. 2002. The retinoblastoma tumour suppressor in development and cancer. Nat Rev Cancer 2:910–917.

Fahham N, Ghahremani MH, Sardari S, Vaziri B, Ostad SN. 2009. Simulation of different truncated p16 forms and in silico study of interaction with Cdk4. Cancer Inform 7:1–11.

Fahraeus R, Lane DP. 1999. The p16(INK4a) tumour suppressor protein inhibits alphavbeta3 integrin-mediated cell spreading on vitronectin by blocking PKC-dependent localization of alphavbeta3 to focal contacts. Embo J 18:2106–2118.

Fahraeus R, Paramio JM, Ball KL, Lain S, Lane DP. 1996. Inhibition of pRb phosphorylation and cell-cycle progression by a 20-residue peptide derived from p16CDKN2/INK4A. Curr Biol 6:84–91.

Frost SJ, Simpson DJ, Clayton RN, Farrell WE. 1999. Transfection of an inducible p16/CDKN2A construct mediates reversible growth inhibition and G1 arrest in the AtT20 pituitary tumor cell line. Mol Endocrinol 13:1801–1810.

Harada H, Nakagawa K, Iwata S, Saito M, Kumon Y, Sakaki S, Sato K, Hamada K. 1999. Restoration of wild-type p16 down-regulates vascular endothelial growth factor expression and inhibits angiogenesis in human gliomas. Cancer Res 59:3783–3789.

Herman JG, Merlo A, Mao L, Lapidus RG, Issa JP, Davidson NE, Sidransky D, Baylin SB. 1995. Inactivation of the CDKN2/p16/MTS1 gene is frequently associated with aberrant DNA methylation in all common human cancers. Cancer Res 55:4525–4530.

Koh J, Enders GH, Dynlacht BD, Harlow E. 1995. Tumour-derived p16 alleles encoding proteins defective in cell-cycle inhibition. Nature 375:506–510.

Li J, Byeon IJ, Ericson K, Poi MJ, O'Maille P, Selby T, Tsai MD. 1999. Tumor suppressor INK4: determination of the solution structure of p18INK4C and demonstration of the functional significance of loops in p18INK4C and p16INK4A. Biochemistry 38:2930–2940.

Li W, Fan J, Hochhauser D, Banerjee D, Zielinski Z, Almasan A, Yin Y, Kelly R, Wahl GM, Bertino JR. 1995. Lack of functional retinoblastoma protein mediates increased resistance to antimetabolites in human sarcoma cell lines. Proc Natl Acad Sci U S A 92:10436–10440.

McConnell BB, Gregory FJ, Stott FJ, Hara E, Peters G. 1999. Induced expression of p16(INK4a) inhibits both CDK4- and CDK2-associated kinase activity by reassortment of cyclin-CDK-inhibitor complexes. Mol Cell Biol 19:1981–1989.

McDonald NQ, Peters G. 1998. Ankyrin for clues about the function of p16INK4a. Nat Struct Biol 5:85–88.

Michaely P, Bennett V. 1993. The membrane-binding domain of ankyrin contains four independently folded subdomains, each comprised of six ankyrin repeats. J Biol Chem 268:22703–22709.

Obexer P, Hagenbuchner J, Rupp M, Salvador C, Holzner M, Deutsch M, Porto V, Kofler R, Unterkircher T, Ausserlechner MJ. 2009. p16INK4A sensitizes human leukemia cells to FAS- and glucocorticoid-induced apoptosis via induction of BBC3/Puma and repression of MCL1 and BCL2. J Biol Chem 284:30933–30940.

Ortega S, Malumbres M, Barbacid M. 2002. Cyclin D-dependent kinases, INK4 inhibitors and cancer. Biochim Biophys Acta 1602:73–87.

Paggi MG, Baldi A, Bonetto F, Giordano A. 1996. Retinoblastoma protein family in cell cycle and cancer: a review. J Cell Biochem 62:418–430.

Parry D, Peters G. 1996. Temperature-sensitive mutants of p16CDKN2 associated with familial melanoma. Mol Cell Biol 16:3844–3852.

Pavletich NP. 1999. Mechanisms of cyclin-dependent kinase regulation: structures of Cdks, their cyclin activators, and Cip and INK4 inhibitors. J Mol Biol 287:821–828.

Plath T, Detjen K, Welzel M, von Marschall Z, Murphy D, Schirner M, Wiedenmann B, Rosewicz S. 2000. A novel function for the tumor suppressor p16(INK4a): induction of anoikis via upregulation of the alpha(5)beta(1) fibronectin receptor. J Cell Biol 150:1467–1478.

Ramirez PT, Gershenson DM, Tortolero-Luna G, Ramondetta LM, Fightmaster D, Wharton JT, Wolf JK. 2001. Expression of cell-cycle mediators in ovarian cancer cells after transfection with p16(INK4a), p21(WAF1/Cip-1), and p53. Gynecol Oncol 83:543–548.

Roninson IB. 2003. Tumor cell senescence in cancer treatment. Cancer Res 63:2705–2715.

Russo AA, Tong L, Lee JO, Jeffrey PD, Pavletich NP. 1998. Structural basis for inhibition of the cyclin-dependent kinase Cdk6 by the tumour suppressor p16INK4a. Nature 395:237–243.

Serrano M. 1997. The tumor suppressor protein p16INK4a. Exp Cell Res 237:7–13.

Smith-Sorensen B, Hovig E. 1996. CDKN2A (p16INK4A) somatic and germline mutations. Hum Mutat 7:294–303.

Tang KS, Fersht AR, Itzhaki LS. 2003. Sequential unfolding of ankyrin repeats in tumor suppressor p16. Structure 11:67–73.

Tang KS, Guralnick BJ, Wang WK, Fersht AR, Itzhaki LS. 1999. Stability and folding of the tumour suppressor protein p16. J Mol Biol 285:1869–1886.

Tevelev A, Byeon IJ, Selby T, Ericson K, Kim HJ, Kraynov V, Tsai MD. 1996. Tumor suppressor p16INK4A: structural characterization of wild-type and mutant proteins by NMR and circular dichroism. Biochemistry 35:9475–9487.

Villacanas O, Perez JJ, Rubio-Martinez J. 2002. Structural analysis of the inhibition of Cdk4 and Cdk6 by p16(INK4a) through molecular dynamics simulations. J Biomol Struct Dyn 20:347–358.

Weinberg RA. 1995. The retinoblastoma protein and cell cycle control. Cell 81:323–330.

Whitaker NJ, Bryan TM, Bonnefin P, Chang AC, Musgrove EA, Braithwaite AW, Reddel RR. 1995. Involvement of RB-1, p53, p16INK4 and telomerase in immortalisation of human cells. Oncogene 11:971–976.

Xie QC, Hu YD, Wang LL, Chen ZT, Diao XW, Wang ZX, Guan HJ, Zhu B, Sun JG, Duan YZ, Chen FL, Nian WQ. 2005. The co-transfection of p16(INK4a) and p14(ARF) genes into human lung cancer cell line A549 and the effects on cell growth and chemosensitivity. Colloids Surf B Biointerfaces 46:188–196.

Yang R, Gombart AF, Serrano M, Koeffler HP. 1995. Mutational effects on the p16INK4a tumor suppressor protein. Cancer Res 55:2503–2506.

Yang R, Serrano M, Slater J, Leung E, Koeffler HP. 1996. Analysis of p16INK4a and its interaction with CDK4. Biochem Biophys Res Commun 218:254–259.

Yarbrough WG, Buckmire RA, Bessho M, Liu ET. 1999. Biologic and biochemical analyses of p16(INK4a) mutations from primary tumors. J Natl Cancer Inst 91:1569–1574.

Yuan C, Li J, Selby TL, Byeon IJ, Tsai MD. 1999. Tumor suppressor INK4: comparisons of conformational properties between p16(INK4A) and p18(INK4C). J Mol Biol 294:201–211.

Zhang B, Peng Z. 2000. A minimum folding unit in the ankyrin repeat protein p16(INK4). J Mol Biol 299:1121–1132.

Zhang B, Peng ZY. 2002. Structural consequences of tumor-derived mutations in p16INK4a probed by limited proteolysis. Biochemistry 41:6293–6302.